# A MULTI-RESOLUTION WAVELET ANALYSIS OF THE RELATIONSHIP BETWEEN THE SOLAR SUNSPOT NUMBER AND THE GEOMAGNETIC INDEX AA

**Silvia Duhau*** **and Charles Y. Chen#**
*Laboratorio de Geofísica, Departamento Física, Ciudad Universitaria, Pabellón I, 1428, Buenos Aires, Argentina
#School of Electrical Engineering, Cornell University, 306 Rhodes Hall, Ithaca N Y, 14853, U.S.A.
duhau@df.uba.ar

Está ampliamente aceptado que la actividad solar en cada máximo está relacionada con la actividad geomagnética en el mínimo precedente. Eso implica que debe existir una relación a largo plazo entre los índices que las miden. En el presente trabajo se estudia esta relación mediante la aplicación de un análisis multi-resuelto basado en la transformada de ondeletas, a la serie temporal del índice geomagnético aa y del número de manchas solares desde el año 1844 al presente. A diferencia de la transformada de Fourier, la metodología empleada permite describir tanto fenómenos periódicos como transitorios y por lo tanto detectar ciclos cuya longitud varía en el tiempo.
Se encuentra que las variaciones temporales de Rz y de aa pueden separase en tres escalas distintas: la escala mas corta corresponde para Rz al bien conocido ciclo de 11 años –ciclo de Schwabe - y las variaciones temporales en las otras dos escalas tienen propiedades que permiten identificarlas con el ciclo de Hale y el de Gleissberg, respectivamente.

It is widely accepted that the solar activity at its maximum is related to geomagnetic activity at a preceding minimum. Therefore, there must exist a relationship in the long term between the indices that measures them. In this paper, we study this relationship by applying a multi-resolution analysis, via the wavelet transform, on the time series of the aa geomagnetic index and the solar sunspot number. While only periodic phenomena may be studied adequately with the Fourier transform, wavelet transform is suitable for describing periodic as well as transient phenomenon.
We found that the temporal variation of Rz may be separated into three different scales: a short scale corresponding to the 11-year Schwabe cycle, and two longer ones with properties such that one identifies with the Hale while the other with the Gleissberg cycle

## I. INTRODUCTION

Geomagnetic activity at its minimum is indicative of the sun's polar magnetic field strength[1,2]. Ohl[3] found a close link between the geomagnetic minimum and the sunspot maximum following that minimum. This link between the two activities may be explained by a dynamo mechanism[4], which, at the start of a Schwabe cycle, transforms the sun's polar field into an internal toroidal field that years later increases during the maximum phase of the Schwabe cycle.

By examining the eleven-year average of the aa index, Russell[5] and Russell and Mulligan[6] have found that there are long-term changes in geomagnetic activity. They believe that these changes imply the existence of long-term variations in the sun's polar magnetic field that are related to changes in the sun on the same temporal scale. On the other hand, a strong positive correlation between the eleven-year running mean of proxy data such as the Zurich sunspot number (Rz), Ap, Dst[7] and aa indices[8,9] have been found. This correlation indicates that, due to the above mentioned dynamo mechanism, the long-term changes in the polar and toroidal solar field are related and these changes are reflected in the geomagnetic and solar activities.

The literature mentions two long-term cycles in solar activity: the Hale and the Gleissberg cycles; both are seen in the qualitative behavior of the Rz time series. The "Gleissberg" cycle is seen in the envelope of the annual average of Rz; the "Hale" cycle is seen in the fact that stronger and weaker Schwabe cycles often alternate (see e. g. ref. 10 to 12).

Since the long term behavior of the geomagnetic and solar activities are related to the polar and the toroidal phases of the Sun's magnetic field, respectively, we expect that their proxy data manifest the Hale and the Gleissberg cycles. To investigate this, we chose to analyze the geomagnetic index aa and solar sunspot number Rz, since these are the longest running indices of geomagnetic and solar activity, respectively.

Quantitative representations of the Hale and the Gleissberg cycles are still lacking. Conventional methods of time series analysis, such as Fourier transform, are designed to analyze periodic phenomena; these methods are unsuitable for the study of time series that contains transient and quasi-periodic phenomena, such as ones related to solar activity. Wavelet analysis, however, is more suitable, for it allows one to decompose transient as well as cyclical phenomena (see e. g. ref. 13,14). In this paper we chose the Morlet wavelet (a Gaussian wave packet with a unique Fourier period) to analyze the long-term behavior in aa and Rz indices.

## II. WAVELET ANALYSIS

There are very good tutorial papers about the applications of the wavelet transform to the analysis of time series (see e. g. ref. 15 and 16); therefore, we will only present a brief summary of the principal elements.

The wavelet transform is defined by:

$$Wf(\lambda,t)=\int_{-\infty}^{\infty} f(u)\overline{\psi}_{\lambda,t}(u)du\,, \qquad \lambda>0, \qquad (1)$$

where:

$$\psi_{\lambda,t}(u) \equiv \frac{1}{\lambda^{1/2}} \psi\left(\frac{u-t}{\lambda}\right) \qquad (1.1)$$

is the wavelet function, that we have selected to be the Morlet wavelet -a gaussian wave packet– and $\lambda$, the scale, a dimensionless frequency related to the Fourier period by .

$$T = \frac{4\pi\lambda}{k + \sqrt{2+k^2}} \qquad (2)$$

The study of the relationship between the wavelet transform wave, i.e., the wavelet coefficient, at each scale (Fourier period) will give information concerning the relationship between two time series. This is called multi-resolution analysis[16].

The set of wavelet coefficients as a function of time and scale can be represented by a scalogram. The scalogram shows the temporally - or spatially - varying localized energy spectrum. On the other hand, if, for a given scale, we integrate the scalogram at each scale, we can compute the spectrogram, which represents, as in the Fourier analyses, the average strength contained in a given Fourier period. Note a Fourier equivalent of the scalogram does not exist, since in Fourier analysis we assume that the energy contained in a given scale (frequency) is constant in time.

To compute the wavelet transform, we divide the scale domain into octaves, which are logarithmic with the base of two. In other words, the scale parameter $\lambda$ is redefined to be

$$\lambda = \lambda_0 2^{n/\nu} \qquad n = 1, 2, \ldots n_0 \qquad (3)$$

where $\lambda_0$ is the smallest resolvable scale, $\nu$ is the number of voices to be included between octaves and $n_0$ the number of octaves, given by:

$$n_0 = \log_2 (N\delta t / \lambda_0) \qquad (3.1)$$

where N is the number of points in the time series with sampling period $\delta t$. This selection allows us to include a broad range of scales, from very small to very large, in an efficient way in a coordinate system with linear interval in octave while logarithmic in scale (frequency). If a larger scale decomposition is desired, each octave may be further subdivided into infinitely many voices. Practically, the voices are finitely chosen so that the scale ratio between any two consecutive voices in the wavelet domain is fixed[15].

## III. RESULTS

### Wavelet reconstruction of the time series

The wavelet transform is, in a sense, the convolution of the signal with a wavelet of a given scale $\lambda$. We can reconstruct the function by simply summing the results of the convolution for all of the scales in the decomposition. We can do this because of the symmetry of the Morlet wavelet. We have selected $\lambda_0 = 2.833$ so that the third octave corresponds to. T = 10.7 years, the average period of the Schwabe cycle for the period considered (1844 to 1997) This procedure leads to a suitable scale resolution and allows an almost perfect reconstruction of the time series. The length of the signal allows us to decompose it into 13 scales (octaves) when we take $k = 4$.

To find the wavelet transform waves of the time series, we first subtract a linear trend from the data and then apply Equation (1) to the result. By this procedure we find 13 waves, one for each of the selected scales (Fourier periods). Summing them and adding the trend, we can reconstruct the time series. The result is shown in Fig. 1. The relative difference between the original and the reconstructed time series is less than 5%. Increasing the number of voices does not substantially decrease this difference. The accuracy of the representation is instead

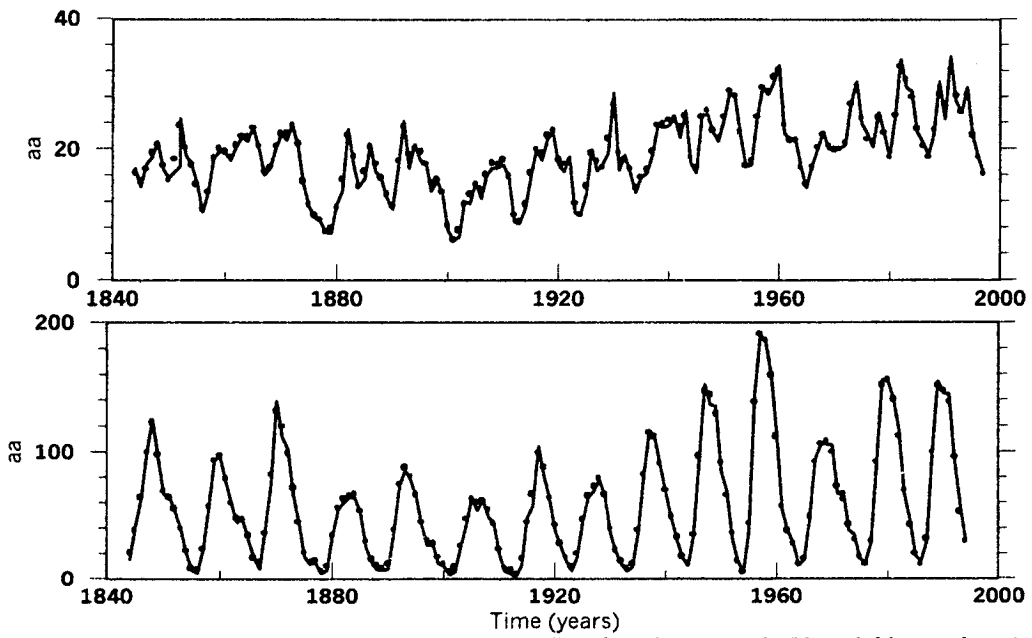


*Figure 1. The time series of the yearly average of aa (upper panel) and Rz (lower panel). The solid line is the original data while the dotted line is the time series reconstructed from the wavelet decomposition. The National World Data Center A[17] supplied the aa data from 1973-to present and the Rz data. Aa data for the periods 1700-1867 and 1868-1973 are from Nevanlinna and Katoja[18] and Mayaud[19], respectively.*

dependent on the value of $k$ chosen for the wavelet.

## The scalogram

Fig. 2 shows the scalograms of Rz and aa. A white spot indicates a maximum and a black a minimum. Therefore, a regular sequence of white and black spots indicates the presence of a cycle. Three cycles are apparent in the scalogram. One for periods below about 15-years, which corresponds to the well-known Schwabe cycle, whose period may be directly evaluated from the time series of Rz (see fig. 1), and other two between 15 to 70 years – decadal scale - and above 70 years – secular scale-, respectively.

In short, the scalogram indicates the presence of three cycles in the time span considered. A quantitative determination of the scales contained in each of them is performed in the next section

## Multi-resolution analysis

Of the 13 wavelet transform waves which, together with the previously removed linear trend, allow us to reconstruct the time series, five correspond to the Schwabe cycle and four to each of the other two cycles.

The top panels in Fig. 3a and 3b show the wavelet transform waves for Rz that correspond to the decadal and the secular cycles, respectively. A similar set of waves exists for the aa time series. The bottom panels show the decadal (fig. 3a) and secular (fig. 3b) cycles for aa and Rz, respectively, as reconstructed from the corresponding wavelet transform waves.

The wavelet transform waves within the decadal cycle have Fourier periods ranging from 22 to 45 years (fig. 3a, upper panel); the reconstruction yields a signal with a smaller variation in the period of the decadal cycle (fig. 3a, lower panel). Prior to 1910, the decadal cycle has a period of around 26 years and since 1910 the period has increased suddenly to about 34 years. In synchronicity to this change in the periodicity of the cycle, there is a

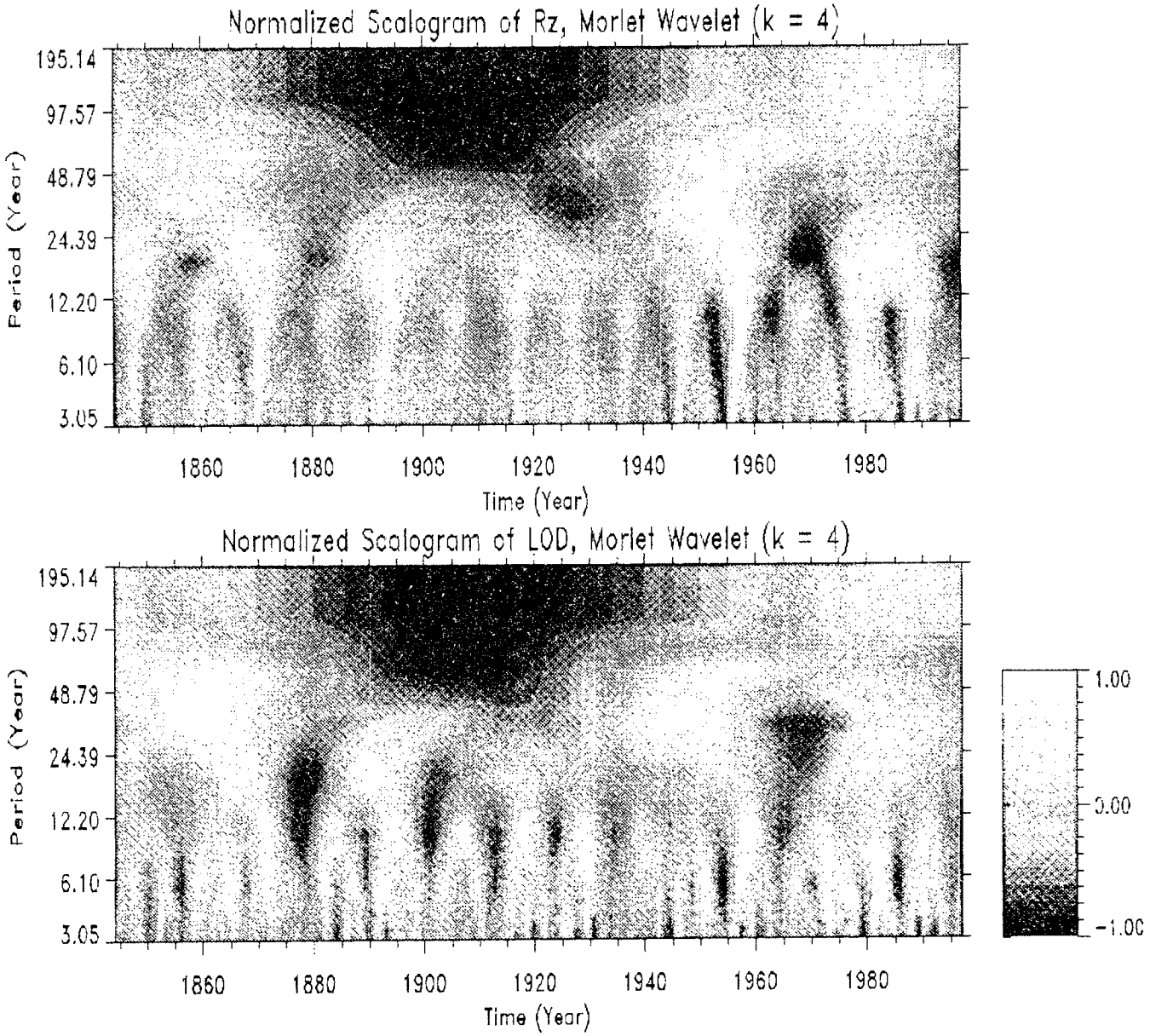


*Figure 2. The scalograms of the aa and Rz data shown in Fig. 1.*

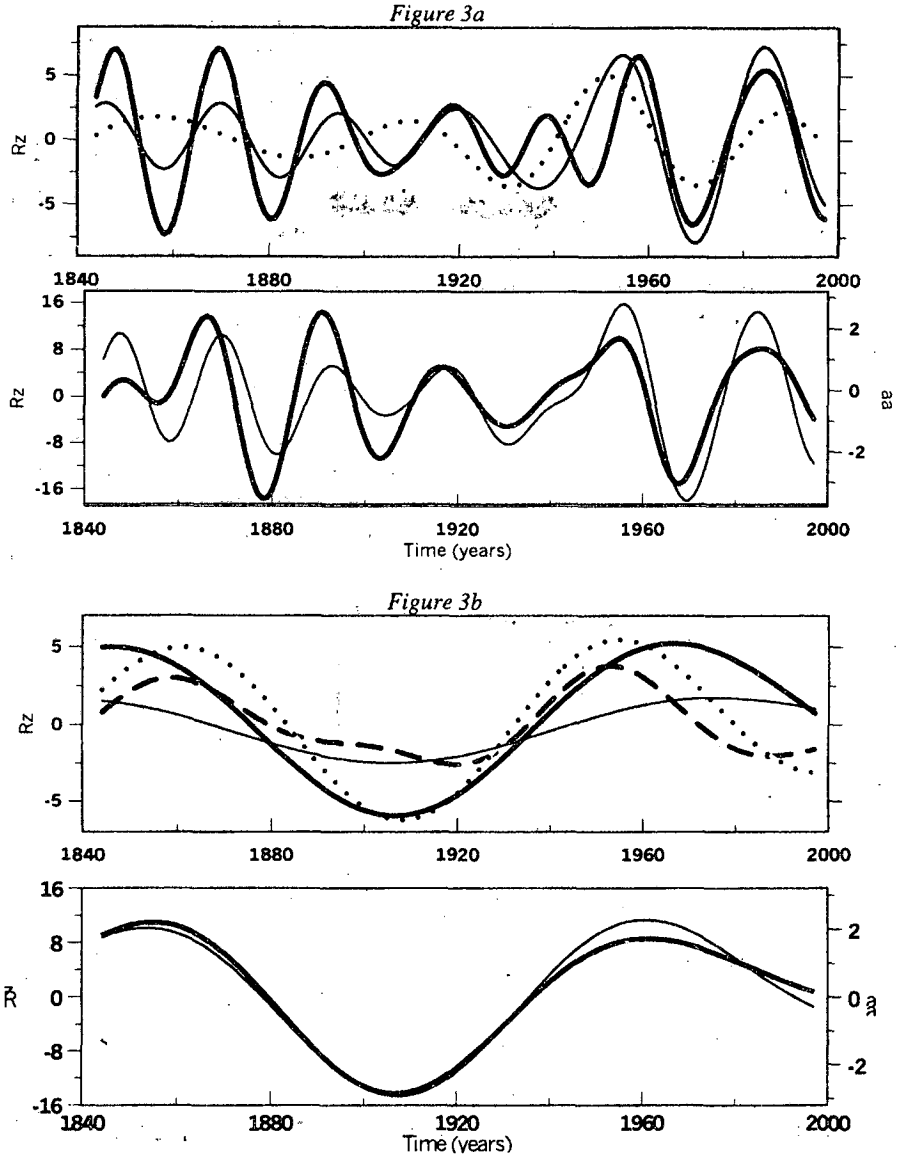


*Figure 3. The wavelet decomposition for the decadal (Fig. 3a) and the secular (Fig. 3b) time scales. In Fig.s 3a and 3b, the wavelet transform waves of those time scales are shown in the upper panel. The corresponding reconstruction of Rz (thin line) as well as for aa (thick line) in those time scales is shown in the lower panel.*

variation in the relative amplitude of the signals: the amplitude Rz is larger than the amplitude of aa after 1910.

The waves that conform to the secular cycle have Fourier periods ranging form 70 to 170 years (Fig. b, upper panel) but lead to a cycle ( Fig b, lower panel) that have an smaller variation in period: increasing from 90 years at the beginning of the time series to 100 years at the end. Also, the amplitude of the secular cycle is quite constant with time. A puzzling feature is the abrupt change in the decadal cycle that occurs when the secular cycle is passing through a minimum (compare lower panels in Fig. 3a and 3b).

## IV. ANALYSIS OF THE RESULTS

Fig. 4 shows the time series of Rz together with the decadal and the secular time variations. To get the secular variation we have added the tendency to the secular cycle. The magnitude of the secular variation follows the envelop of the peaks of the Rz time series, and the relative amplitude of the maxima of two successive Schwabe cycle are followed by the decadal cycle. So these variations have the qualitative features by which the Hale and the Gleissberg cycles have been recognized in the Rz time series[10, 11, 12].

Therefore, we may identify the secular and the decadal cycles with the so-called Hale and the Gleissberg cycles, respectively. According to Rusell[5] and Russel and Mulligan[6], long-term changes in geomagnetic indices may be interpreted as changes in the strength of the polar field of the sun. Also, solar activity during a Schwabe cycle is proportional to the toroidal field strength[4]. Therefore, we may interpret the Hale and the Gleissberg cycles in aa and Rz in terms of the long-term evolution of the solar magnetic field.

Fig. 5 shows the spectrogram, the wavelet version of a power spectrum, of aa and Rz for the time period prior to 1910 and afterward. The peaks in the spectrogram correspond to the periods of the dominant wavelet transform waves (the ones shown in the upper panel of

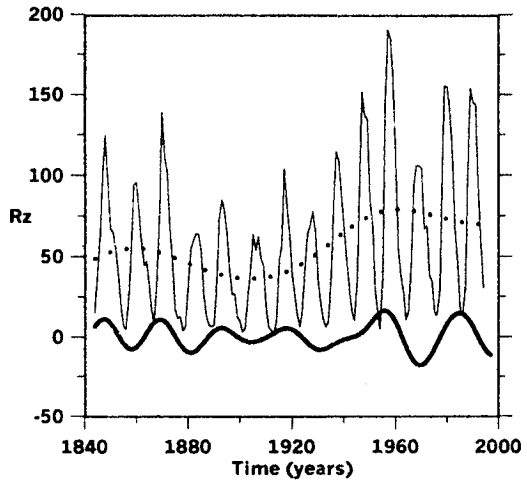


*Figure 4. The solar sunspot number (Rz) (thin line) and the Hale (thick line) and the Gleissberg cycles (dotted line), respectively.*

fig. 3a). Therefore, this result indicates that the energy of the decadal cycle has shifted suddenly from the shorter to the longer scales around year 1910. This redistribution of the energy between dominant waves occurred when the Gleissberg cycle (bottom panel in Fig. 3b) was passing by a minimum. Also, aa and Rz simultaneously reach a minimum at 1910 (see Fig. 3a, bottom panel), the year during which the number of sunspots was 5, the smallest on the time span considered (see Fig. 4). Finally, the relative energy contained in Rz as compared with aa increases suddenly after 1910.

Since aa and Rz are a measure of the poloidal and the toroidal field of the sun, respectively, we may interpret the above result in terms of the components of the sun's magnetic field. The length of the Hale cycle increases (decreases) with increasing (decreasing) toroidal (poloidal) component of the sun's magnetic field, and the relative strength of the toroidal field with respect to that of the poloidal one has increased suddenly after 1910.

*Acknowledgements: This work was performed when one of the authors (Silvia Duhau) was visiting the School of Electrical Engineering Department at Cornell University. This author wants to express her profound gratitude to the Fulbright Commission for their support that made it possible and to Prof. Michael Kelley for his kind hospitality.*

*This work was supported by the Buenos Aires University, the National Agency of Promotion of Science and Technology and the National Council of Scientific and Technical Research, under Grant II05, PIC 00-00551 and 4490, respectively.*

## References

1. Layden, A. C., P. A. Fox, J. M. Howard, A Sarajedini, K. H. Schatten and S. Sofia, Solar Physics, 132, 1, 1991
2. Legrand, J. P. and Simon, P. A., Solar Phys., 131, 187, 1991.
3. Ohl, A. I.: 1966, Soln. Dann. Nro. 12, 84.
4. Babcock, H. W., Astrophysics. J., 133, 572-587, 1961
5. Russell, C. T., Geophys. Res. Let., 1, 11-12, 1974.
6. Russell, C. T. and T. Mulligan, Geophys. Res. Let., 1-23, 1988.
7. Duhau S, and E., A. Martínez E., Geophys. Res. Let, 22, 3283-3288, 1995
8. Duhau, S. and E. A. Martínez, Actas de la 19ª Reunion Cientifica de Geofisica y Geodesia, 86-89, 1997.
9. Duhau, S., and Martínez, E., EOS 79, Spring Meet. Suppl., S290, 1998.
10. Foukal, P. V., Solar Astrophysics, pp. 476, Wiley, New York, 1990.
11. Hoyt D. and K. H. Schatten, The role of the sun and climate change, pp.279, Oxford, New York, 1997.
12. Eddy, J. A., Secular, Solar and Geomagnetic Variations in the Last 10,000 Years, F. R. Stephenson and A. W. Wolfendale (Eds.), Kluwer Academic Publishers, NATO ASI Series C.
13. Lau, K. M. and Weng, H., Bull. Am. Meteorol. Soc, 2391-2402, 1995.
14. Alcala, Christian M., Radar Scattering from Nonturbulent Layers in the Summer Polar Mesosphere, Ph.D. Thesis, pp. 238, Cornell University, N.Y., May 1998.
15. Daubechies, I., Ten lectures on wavelets, CBMS-NSF Regional Conference Series in Applied Mathematics, S.I.A.M., 61, 1988.
16. Mallat, S. Multiresolution approximation and wavelet orthonormal basis in L2(R). Trans. Amer. Math. Soc. 315, 69-87 (1989).
17. Word Data Cent. A Sol.-Terr. Phys., Boulder Colo.
18. Nevanlinna, H and E. Katoja, Geophys. Res. Let., Geophys. Res. Lett., 20, 2703, *1993*
19. Mayaud, P. N., IAGA Bulletin, 33, 1868-1978, 1973.

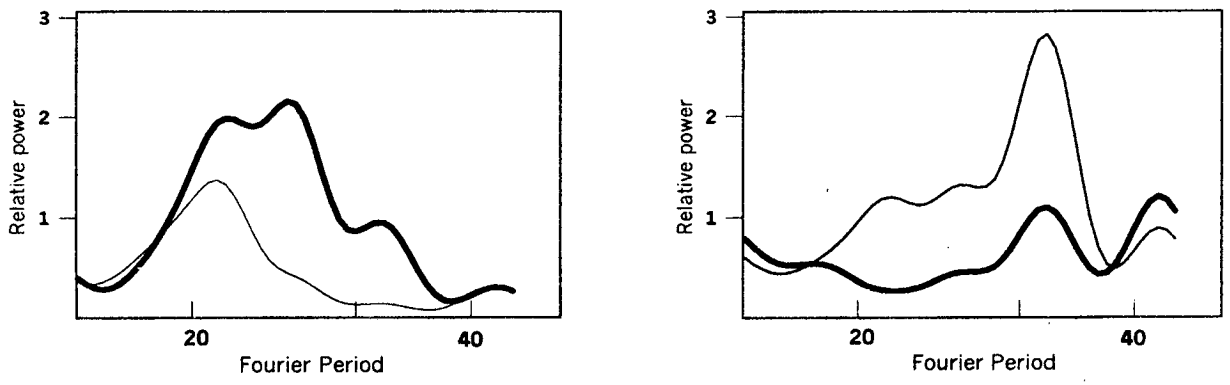


*Figure 5. Wavelet power spectrum of aa (thick line) and Rz (thin line) for the periods 1844-1910 (left) and 1911-1997 (right)*